Development 133, 163-171 doi:10.1242/dev.02177

Drosophila Knickkopf and Retroactive are needed for epithelial tube growth and cuticle differentiation through their specific requirement for chitin filament organization

Bernard Moussian[1,*,†], Erika Tång[2,*], Anna Tonning[2], Sigrun Helms[1], Heinz Schwarz[1], Christiane Nüsslein-Volhard[1] and Anne E. Uv[2,†]

Precise epithelial tube diameters rely on coordinated cell shape changes and apical membrane enlargement during tube growth. Uniform tube expansion in the developing *Drosophila* trachea requires the assembly of a transient intraluminal chitin matrix, where chitin forms a broad cable that expands in accordance with lumen diameter growth. Like the chitinous procuticle, the tracheal luminal chitin cable displays a filamentous structure that presumably is important for matrix function. Here, we show that *knickkopf* (*knk*) and *retroactive* (*rtv*) are two new tube expansion mutants that fail to form filamentous chitin structures, both in the tracheal and cuticular chitin matrices. Mutations in *knk* and *rtv* are known to disrupt the embryonic cuticle, and our combined genetic analysis and chemical chitin inhibition experiments support the argument that Knk and Rtv specifically assist in chitin function. We show that Knk is an apical GPI-linked protein that acts at the plasma membrane. Subcellular mislocalization of Knk in previously identified tube expansion mutants that disrupt septate junction (SJ) proteins, further suggest that SJs promote chitinous matrix organization and uniform tube expansion by supporting polarized epithelial protein localization. We propose a model in which Knk and the predicted chitin-binding protein Rtv form membrane complexes essential for epithelial tubulogenesis and cuticle formation through their specific role in directing chitin filament assembly.

KEY WORDS: Tubulogenesis, Trachea, Epidermis, Cuticle, Chitin, *Drosophila*, Apical ECM, Knk, Septate junction

INTRODUCTION

Chitin, cellulose and hyaluronan are abundant polysaccharides that provide mechanical tissue stability to arthropod and fungal exoskeletons, plant cell walls and vertebrate supporting tissues. Over recent years, the functions of these polymers have been found also to include developmental and morphogenetic cues. Hyaluronan regulates cell behaviour during embryonic development (Bakkers et al., 2004; Spicer and Tien, 2004; Toole, 2004), and cellulose fibre orientation in plants controls the directionality of cell expansion (Roudier et al., 2005). In addition, an essential role for chitin in epithelial tube size regulation in the developing fly trachea was recently discovered (Tonning et al., 2005). The tracheal system stems from epithelial sacks that invaginate from the epidermis and ramify to generate tubes of distinct dimensions (Ghabrial et al., 2003; Uv et al., 2003). Like many developing tubes, the newly formed tracheal branches are narrow, and subsequent tube expansion to attain functional lumen sizes requires coordinated cell rearrangements and apical membrane growth (Beitel and Krasnow, 2000). Tracheal chitin is synthesized and deposited into the lumen by Chitin synthase 1 (CS-1), and loss of tracheal chitin causes severe lumen diameter irregularities, with local dilations and cysts. Luminal chitin assembles into a defined transient cable that expands in unison with lumen diameter growth, suggesting that the shape and organization of the chitin matrix is crucial for uniform tube growth (Tonning et al., 2005).

[1]Department of Genetics, Max-Planck-Institute for Developmental Biology, Tübingen, Germany [2]Department of Medical Biochemistry, Gothenburg University, Gothenburg, Sweden.

*These authors contributed equally to this work
[†]Authors for correspondence (e-mail: anne.uv@medkem.gu.se; bernard.moussian@tuebingen.mpg.de)

Accepted 25 October 2005

Chitin is a long linear sugar formed by transmembrane enzymes that link cytosolic UDP-N-acetyl-D-glucosamine (UDP-GlcNAc) into chains of repeating GlcNAc residues that extrude from the apical cell surface (Cohen, 2001). CS-1 is encoded by *krotzkopf verkehrt* (*kkv*) and is responsible for chitin deposition also in the embryonic cuticle (Ostrowski et al., 2002; Moussian et al., 2005a). Within the stratified cuticle, chitin is found as a lamellar structure in the layer abutting the epidermal cells, called the procuticle. These lamellae are built from sheets of chitin microfibrils and are tightly packed to confer stability and elasticity to the exoskeleton, as well as assisting in the concurrent deposition of the overlaying protein-rich epicuticle (Merzendorfer, 2005; Moussian et al., 2005a). The architecture of the tracheal luminal chitin matrix is not known, but here chitin also appears organized into long filaments that run parallel with tube length (Tonning et al., 2005). Many previously identified tracheal tube expansion mutants exhibit an abnormal intraluminal chitin fibre, where matrix diameter and texture are affected (Tonning et al., 2005). These mutants disrupt genes that encode septate junction (SJ) proteins (Behr et al., 2003; Paul et al., 2003; Llimargas et al., 2004; Wu et al., 2004) and develop overgrown tracheal lumens. SJs share some functions and components with vertebrate tight junctions, but localize to the lateral cell surface, and their requirements for luminal chitin fibre organization and tube expansion are unclear (Wu and Beitel, 2004).

In order to understand more about chitin matrix assembly and regulated tracheal tube expansion, we tested whether mutations known to disrupt cuticle differentiation could affect the tracheal luminal chitin matrix. Here we show that the two mutants *knickkopf* (*knk*) and *retroactive* (*rtv*), which display cuticle phenotypes that parallel that of *krotzkopf verkehrt* (*kkv*) (Jurgens et al., 1984; Wieschaus et al., 1984; Ostrowski et al., 2002; Moussian et al., 2005a), develop severe tracheal tube size defects that are reminiscent of those of chitin-deficient embryos. Rtv encodes a transmembrane

protein with putative chitin-binding properties and is required for lamellar procuticle organization (Moussian et al., 2005b). We find that Knk and Rtv are specifically required for chitin filament assembly in the tracheal lumen and cuticle. Further analysis of Knk uncovers an essential role for the tracheal epithelium in organizing extracellular chitinous matrices.

MATERIALS AND METHODS

Immunohistochemistry

Embryos were fixed and stained as described (Samakovlis et al., 1996), unless otherwise noted. The following primary antibodies were used: tracheal lumen specific antibody mouse monoclonal IgM 2A12 [1:10; Developmental Studies Hybridoma Bank (DSHB)], rabbit anti-β-gal (1:500; Jackson), rabbit anti-GFP (1:500; Molecular Probes), mouse IgG1 monoclonal anti-Crumbs (1:10; DSHB), rabbit IgG anti-Pio (1:20; provided by M. Affolter), mouse IgG monoclonal anti-Discs large 1 (1:10; DSHB) and mouse monoclonal IgG2a anti-Fasciclin 3 (1:10;DSHB). The Knk antiserum was generated by immunizing rabbits with a fusion protein containing amino acids 33 to 484 of Knk fused to a His-tagged polypeptide (Qiagen). The anti-Knk antiserum was pre-absorbed against wild type embryos (stages 0-13) before use (1:1500). For fluorescent visualization the following secondary antibodies from Molecular Probes were used at 1:500 dilution: Alexa 488 goat anti-rabbit IgG, Alexa 488 goat anti-mouse IgM, Alexa 594 goat anti-mouse IgM, Alexa 546 goat anti-mouse IgG, Alexa 546 goat anti-rabbit IgG, Alexa 555 goat anti-mouse IgG and Alexa 555 goat anti-rabbit IgG.

For labelling of tracheal luminal chitin, embryos were incubated with a FITC-conjugated chitin-binding probe (CBP; New England BioLabs) at 1:500 dilution for 3 hours together with the secondary antibody, and mounted in Prolong anti-fade (Molecular Probes). A BIO RAD RADIENCE 2000 was used to obtain confocal images, and Nikon Eclipse E1000 was used for obtaining fluorescent images. Images were processed in Adobe Photoshop 7.0.

Fly strains and chemical treatments

The mutant alleles of *kkv*, *knk* and *rtv* used in this study were kkv^{1}, knk^{7A69}, knk^{5C77}, rtv^{11} and rtv^{BNd}, which are amorphic ethyl methanesulfonate (EMS)-induced mutations (Jurgens et al., 1984; Wieschaus et al., 1984; Ostrowski et al., 2002; Moussian et al., 2005b). The other tube expansion mutants used were $mega^{G0012}$ (pck^{G0012} – FlyBase; obtained from Bloomington Stock Collection), $fas2^{EB112}$ (Grenningloh et al., 1991), grh^{s2140} (Spradling, 1999) and grh^{IM}. The UAS-lines *UAS-knk* and UAS-knk^{TM} were generated by standard germline transformation. *UAS-knk* contains the *knk* open reading frame obtained by RT-PCR from pupal extract. *UAS-*knk^{TM} contains a sequence encoding the N-terminal 667 amino acids of Knk (i.e. omitting the last predicted recognition domains required for GPI-modification) fused to a sequence encoding the C-terminal 17 amino acids transmembrane domain of Transferrin (CG10620). Sequences of CG10620 that could code for the predicted recognition domains required for GPI-modification were not included. The two GAL4-lines used were *Btl-Gal4* line (Shiga et al., 1996), which expresses GAL4 in all tracheal cells from stage 12-13, and *Tub-GAL4*, which expresses ubiquitous GAL4. In all experiments *CyO*, *TM3* and *FM7c* balancer strains carrying *GFP* or *lacZ* transgenes were used as necessary to identify embryos with the desired genotypes.

Inhibition of chitin synthesis was achieved with Nikkomycin Z (Sigma-Aldrich). Nikkomycin was diluted in water to generate a stock solution of 10 mg/ml, mixed with heat-inactivated yeast paste (1:10) to generate a final concentration of 1 mg/ml, and placed on a piece of parafilm on apple plates on which the flies could feed. Flies were fed Nikkomycin-containing yeast for 2 days before embryo collections.

In-situ hybridization

Whole-mount in-situ hybridizations were performed with digoxigenin-labelled RNA sense and antisense probes as described (Tonning et al., 2005). RNA probes for *knk* were generated using the *knk* cDNA RE24065 as template, and were hydrolyzed to yield RNA probes of approximately 500 bases.

Histology

Fully developed embryos were dechorionated manually, devitellinized by shaking in 100% methanol, and incubated over night at 65°C in Hoyer's medium mixed with lactic acid (1:1) (Wieschaus and Nüsslein-Volhard, 1986). Embryos were analysed by fluorescence and light microscopy using a Zeiss Axiophot. Transmission electron microscopy (TEM) analysis was performed as described by Moussian and colleagues (Moussian et al., 2005a). For gold labelling of chitin, we used biotinylated Wheat Germ Agglutinin (WGA; 1:500, Vector Laboratories), which was recognized by an anti-biotin antibody (1:300, Enzo Diagnostics), which in turn was detected by protein A conjugated to 10-nm gold particles (1:100). Specimens labelled with gold were contrasted for only 3 minutes instead of 10 minutes.

Molecular biology

For protein sequence analysis and comparisons, tools and software at the Expasy proteomics server were used (http://www.expasy.org). The mutant alleles of *knk* were sequenced using PCR fragments amplified from homozygous *knk* genomic DNA as templates. For each allele at least two independent PCR-reactions were sequenced.

Western blot protein analysis

Larval membrane preparations were prepared with the Pierce Mem-PER Eukaryotic Membrane Protein Extraction Kit using protocol 3 for soft tissue, and detergents were removed using the PAGEprep Advance Kit from Pierce. For western blot experiments, the Knk antiserum was used in a dilution of 1:2000 on 15 μg of embryo extracts, rabbit anti-Tout-velu (Ttv) at 1:1500 and anti Syx1A (DSHB) at 1:5. For detection, we used Western lightning (Perkin Elmer) with a donkey-HRP-conjugated secondary antibody (1:5000, Amersham). Digestion with Phospholipase C from *Bacillus cereus* (Sigma) was performed on membrane extracts from stage 17 embryos and as proposed by the enzyme supplier.

RESULTS

Mutations in *knickkopf* and *retroactive* disrupt uniform tracheal tube expansion

The cuticle phenotypes of *knk* and *rtv* mutants show many parallels with that of *kkv* mutant embryos (Jurgens et al., 1984; Wieschaus et al., 1984; Ostrowski et al., 2002; Moussian et al., 2005a; Moussian et al., 2005b). We therefore asked if *knk* and *rtv* might have additional roles in tracheal tube size regulation. Two predicted *knk* null-alleles (knk^{7A69} and knk^{5C77}) and one *rtv* null allele (rtv^{11}) were analysed for tracheal tube shapes using the tracheal lumen specific antibody 2A12. Indeed, both *knk* and *rtv* mutant embryos develop anomalous tube dimensions without affecting the branch pattern of the tracheal network (Fig. 1A-C).

The 2A12 antigen is expressed by the tracheal epithelium and secreted into the lumen from the onset of tube diameter growth (Beitel and Krasnow, 2000), and in the major dorsal trunks (DT) (where two to six cells surround the lumen circumference; Fig. 1P) the 2A12 antigen is expressed from embryonic stage 14 (Fig. 1D). At this stage the developing trachea in both *knk* and *rtv* mutants display weak and diffuse luminal 2A12 levels, although the typical cellular levels of this expansion marker appear normal (Fig. 1D-F). During the following 3 hours (stage 15), the wild-type DT diameter expands 3- to 5-fold in a highly regulated manner to form uniform tubes (Fig. 1G,P). In both *knk* and *rtv* mutants this tube expansion is impaired; the DT fusion branch lumens, which are formed by specialized toroidal cells (Fig. 1P), do not expand as much as in the wild type (arrows in Fig. 1G-I), and the remaining DT lumen dilate excessively in both mutants to form tubes with a cystic appearance. The degree of DT diameter defects is weaker in *rtv* than in *knk* mutants (compare also Fig. 2B,C). After diameter growth at stage 15, the DTs of both mutants also become excessively elongated and convoluted (Fig. 1J-L). In addition, the narrow and extended ganglionic branches (GB) display discontinuous 2A12 labelling at

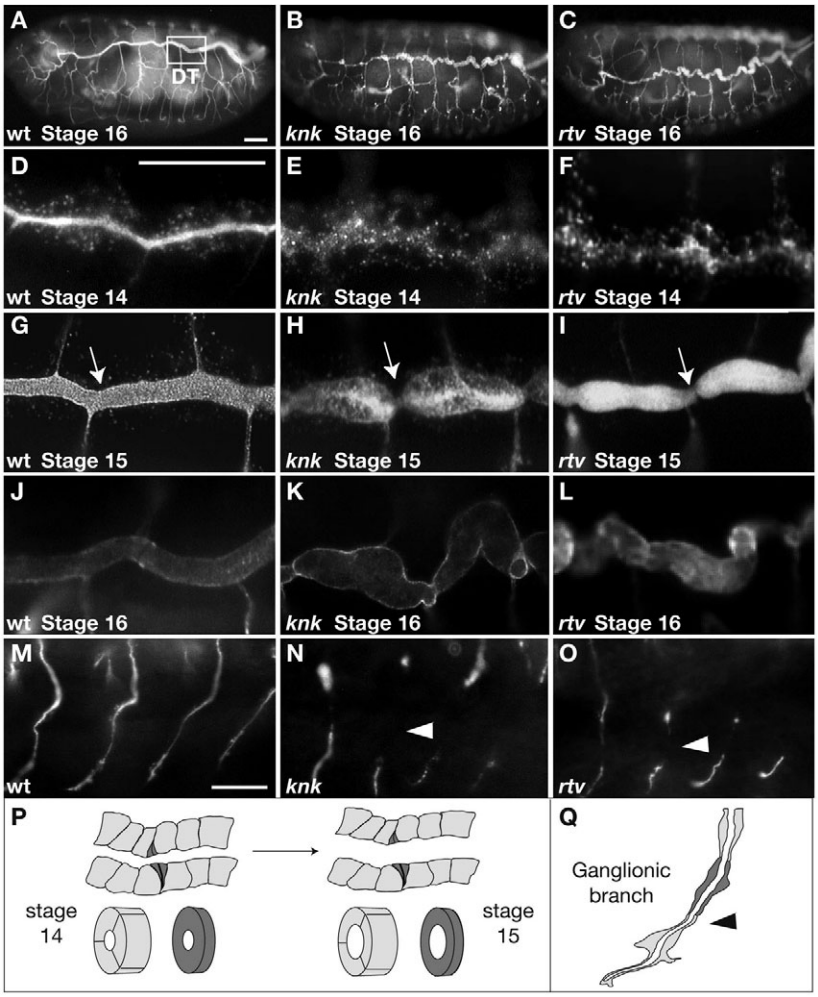

Fig. 1. *knk* and *rtv* are required for uniform tracheal tube expansion. The developing tracheal lumen of wild-type, *knk* and *rtv* mutant embryos was visualized with the lumen-specific antibody 2A12. (**A**-**C**) Stage 16 knk^{7A69} (B) and rtv^{11} (C) mutant embryos display irregular tracheal tube shapes, but no defects in branch patterning, compared with wild-type embryos (A). The box in A depicts the dorsal trunk (DT) region in D-L. (**D**-**F**) At stage 14, the 2A12 antigen begins to accumulate in the wild-type DT lumen (D), but is reduced in the lumen of knk^{7A69} (E) and rtv^{11} (F) mutants. (**G**-**I**) During stage 15, the wild-type DT lumen (G) expands uniformly, whereas the DT lumen of knk^{7A69} (H) and rtv^{11} (I) mutants remain constricted at branch fusions (arrows), and the tube between fusion junctions becomes excessively overgrown. (**J**-**L**) During stage 16, the knk^{7A69} (K) and rtv^{11} (L) mutant DTs in addition become extensively elongated compared with the wild-type trunk (J). (**M**-**O**) The lumen of the narrower multicellular ganglionic branches (GB) is discontinuous in knk^{7A69} (N) and rtv^{11} (O) mutants at the border of the ventral nerve cord (arrowheads), compared with wild type GB (M). (**P**) Illustration of tracheal cell shape changes during DT expansion at stage 15. The DT lumen is encircled by three to five cuboidal cells (pale grey) attached to each other by intercellular junctions, apart from the branch fusion lumens, which are surrounded by two toroidal cells (dark grey). Lumen expansion from stage 14 to 15 does not involve cell division and relies on coordinated growth of the apical cell surfaces. (**Q**) The GB branches are made by rows of single cells folding over themselves, and the arrowhead points to where lumen discontinuities are observed in knk^{7A69} and rtv^{11} mutants. Different shades of grey are used to distinguish neighbouring cells in the row. Scale bars: 25 μm. DT, dorsal trunk.

the entry-point into the ventral nerve cord (arrowheads in Fig. 1M-O,Q), and local lumen dilations are also seen in narrower multicellular tracheal tubes (not shown). Thus, *knk* and *rtv* are two tube size mutants required for (1) uniform tube expansion, (2) restricted tube elongation and (3) lumen integrity in a subset of tracheal epithelial tubes. As lumen dimension relates to the size of the apical epithelial surface, the disrupted tube diameter and lengths in *knk* and *rtv* mutants probably reflects uncoordinated apical cell surface expansion within their tracheal epithelium.

Knk and Rtv are required for tracheal luminal chitin filament assembly

The tracheal phenotypes of *knk* are nearly identical to those of embryos lacking chitin (Tonning et al., 2005), whereas the DT fusion branch constrictions and tube dilations are less severe in *rtv* mutants (Fig. 2B-D). If Knk and Rtv function in a chitin-dependent pathway, the simultaneous disruption of CS-1 activity and either Knk or Rtv would not be predicted to cause enhanced tracheal defects, compared with embryos only lacking chitin. We used the specific chitin synthase inhibitor Nikkomycin, a GlcNAc substrate analogue that acts as a competitive inhibitor of chitin synthases (Cabib, 1991; Tellam et al., 2000) to inhibit chitin synthesis in *knk* and *rtv* mutants. Wild-type flies fed with a Nikkomycin dose of 1 mg/ml produce embryos that reproduce all aspects of the *kkv* mutant phenotype (Fig. 2A,D and not shown). We find that *knk* and *rtv* mutant embryos produced by flies treated with the same Nikkomycin dose develop tracheal defects indistinguishable from those of Nikkomycin-treated wild-type embryos (Fig. 2E,F). Furthermore, by reducing the levels of chitin in wild-type embryos, which was achieved by feeding wild-type parents with a low Nikkomycin dose (0.5 mg/ml), the *rtv* tracheal phenotypes were reproduced (Fig. 2G,H). These results thus correlate with a requirement of Knk and Rtv in a linear pathway with chitin.

The transient intraluminal chitin filament that assembles during the restricted period of lumen expansion can be detected by labelling with a FITC-conjugated chitin-binding probe (CBP) (Tonning et al., 2005). CBP labelling of wild type embryos reveals a luminal chitin fibre that is confined to only part of the lumen and displays a filamentous texture (Fig. 3A). In embryos produced by wild-type parents fed with a high Nikkomycin dose (1 mg/ml) to reproduce the *kkv* phenotype, luminal CBP levels are barely visible (Fig. 3B). We used CBP to assess luminal chitin levels in *knk* and *rtv* mutants, and found that the tracheal lumen of both *knk* and *rtv* mutants label with CBP. However, the luminal chitin in *knk* and *rtv* mutants occupy their entire lumen and display an amorphous texture (Fig. 3C,D).

We also noted that the intensity of the CBP labelling was reduced in *knk* and *rtv* mutant trachea compared with wild type, which may be due to the broader chitin distribution within the mutant lumens. Still, in order to test if *knk* and *rtv* tracheal defects could be due simply to reduced chitin levels, we contrasted the luminal CBP levels of *knk* and *rtv* mutants with that of wild-type embryos treated with a low Nikkomycin dose (0.5 mg/ml) to reproduce the *rtv* tracheal

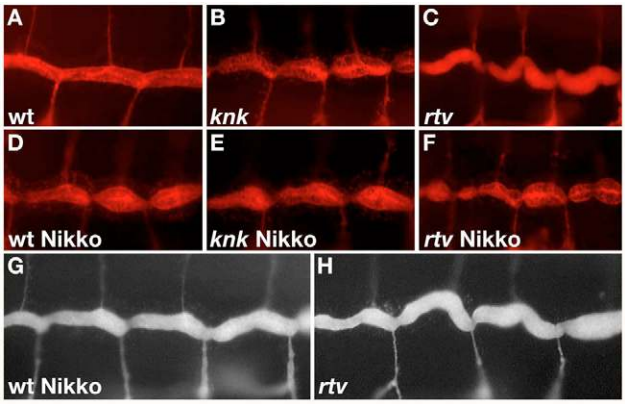

Fig. 2. *knk* and *rtv* functions in the chitin-mediated pathway of tube-size control. (**A**-**F**) Mutations in *knk* and *rtv* do not enhance the tracheal phenotypes of chitin-deficient embryos. Wild-type embryos laid by Nikkomycin-fed parents (1 mg/ml) (D) develop full *kkv* tracheal phenotype with local dilations and cysts, compared with wild type (A). This phenotype is similar to that of knk^{7A69} mutants (B) and to knk^{7A69} mutant embryos laid by Nikkomycin-fed parents (E). Also chitin-deficient rtv^{11} mutant embryos laid by Nikkomycin-fed parents (F) develop tracheal phenotypes indistinguishable from that of chitin-deficient embryos, but the untreated rtv^{11} mutant embryos (C) display less severe tube dilations. (**G**,**H**) When wild-type flies are fed with a low Nikkomycin dose (0.5 mg/ml) (G), their embryonic offspring display tracheal phenotypes reminiscent of the rtv^{11} mutant phenotypes (H). Scale bars: 15 μm in A-F; 20 μm in G,H.

phenotype. Interestingly, chitin diffuse to fill the lumen in embryos with reduced chitin levels also (Fig. 3E), implying that proper chitin filament organization requires a critical level of chitin synthesis. The intensity of the CBP-labelled chitin in these embryos is, however, significantly weaker than in *knk* and *rtv* mutant trachea (compare Fig. 3C-E). In addition, we find that Nikkomycin-treated embryos with milder tracheal defects than that of *knk* and *rtv* mutants also display weaker CBP staining than *knk* and *rtv* mutants (not shown). Thus, Knk and Rtv appear required for chitin filament assembly, rather than chitin synthesis. Another tracheal luminal filament that is required for tracheal cell intercalation to form narrow tubes with auto-cellular junctions contains the PioPio (Pio) protein (Jazwinska et al., 2003). However, the Pio filament is not affected in *knk* and *rtv* mutants (Fig. 6M,N and not shown), implying that Knk and Rtv are required for assembly of only a subset of luminal matrix components.

Knk is needed for chitin filament assembly in the cuticle

Chitin is also a component of the procuticle, the part of the stratified cuticle that adjoins the epidermal cells. As *rtv* mutants lack the lamellar appearance of the procuticle (Moussian et al., 2005b), we asked if *knk* mutants have a similar defect in the organization of the chitinous procuticle. Cuticle preparations of mature *knk* embryos show a dilated cuticle (Fig. 4A,B), and the head skeleton and the pharynx of these embryos are deformed, as the vertical plate is strongly melanized and appear granular instead of fibrous as in the wild-type embryo (insets in Fig. 4A,B). These aspects of the *knk* cuticle are reminiscent of that of *kkv* mutants (Ostrowski et al., 2002; Moussian et al., 2005a). TEM analysis of the *knk* mutant cuticle revealed that the outermost layer of the stratified cuticle, the envelope, appear normal in *knk* mutants, but that the space between the envelope and the epidermal surface is filled with an amorphous substance containing inclusions of electron-dense material, and the typical chitin lamellae appeared absent (Fig. 4C,D). Detection of cuticular chitin with gold-labelled Wheat germ agglutinin (WGA) further show that WGA recognizes chitin in the *knk* mutant cuticle (Fig. 4E,F), whereas WGA labelling is absent in *kkv* mutants (Fig. 4G). We also find that the *rtv* mutant procuticle, which also lacks chitin lamellogenesis, label with WGA (Fig. 4H). Thus, the cuticle defects in *knk* and *rtv* mutants can be explained by their specific requirement in chitin fibril formation.

Knk is an apical GPI-anchored protein that functions at the plasma membrane

The *knk* gene encodes a 689 amino acid protein with unknown function (Ostrowski et al., 2002). The protein is predicted to be extracellular and anchored to the plasma membrane via a GPI moiety (Fig. 5A). Knk also contains two DM13 domains of unknown function and a DOMON domain predicted to form a beta-sandwich structure that is seen in many extracellular adhesion domains, including the fibronectin type III (fn3) domain (Aravind, 2001).

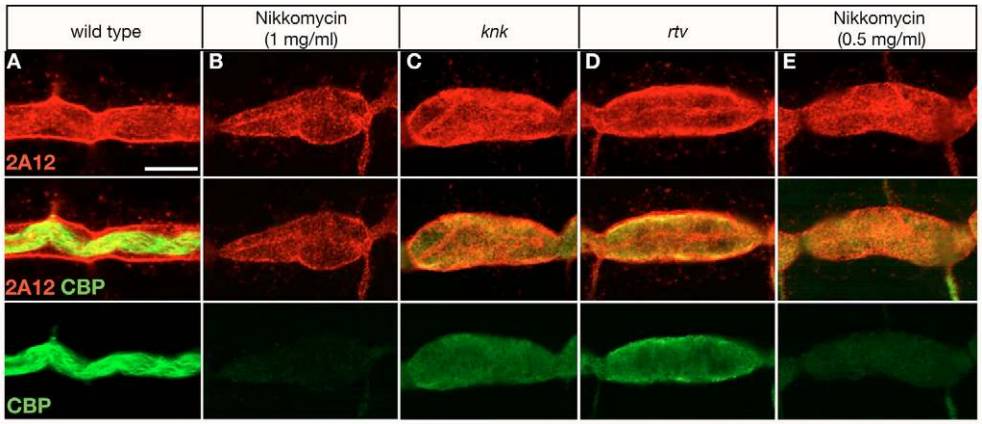

Fig. 3. *knk* and *rtv* are required for tracheal luminal chitin filament assembly. (A-E) Early stage 15 embryos double labelled with luminal antibody 2A12 (red; top panel) and FITC-conjugated chitin-binding probe (CBP; green, bottom panel), where analogous DT segments from each genotype are shown. All embryos were fixed and labelled in parallel and the confocal images taken in the same session with identical settings to display comparative levels of luminal chitin. (In the middle merged panel, colour levels are adjusted to enable visualization of both 2A12 and CBP labelling.) (**A**) In wild-type embryos, CBP labels a luminal chitinous fibre with 'threads' running parallel to tube length. The merged image shows that the CBP-labelled fibre is confined to only a part of the lumen, leaving narrow gaps to the surrounding epithelium. (**B**) The trachea of wild-type embryos laid by Nikkomycin-fed parentsdisplay *kkv* phenotype and barely detectable luminal CBP levels. (**C**,**D**) In both knk^{7A69} (C) and rtv^{11} (D) mutant trachea, CBP labelling reveals a broad chitinous matrix, which fills the entire lumen. (**E**) The intensity of this CBP labelling is weaker than in the wild type, but stronger than in embryos with reduced CS-1 activity upon treatment with a low Nikkomycin dose (0.5 mg/ml) to reproduce the *kkv* and *rtv* mutant phenotypes. Scale bars: 5 μm in A-E.

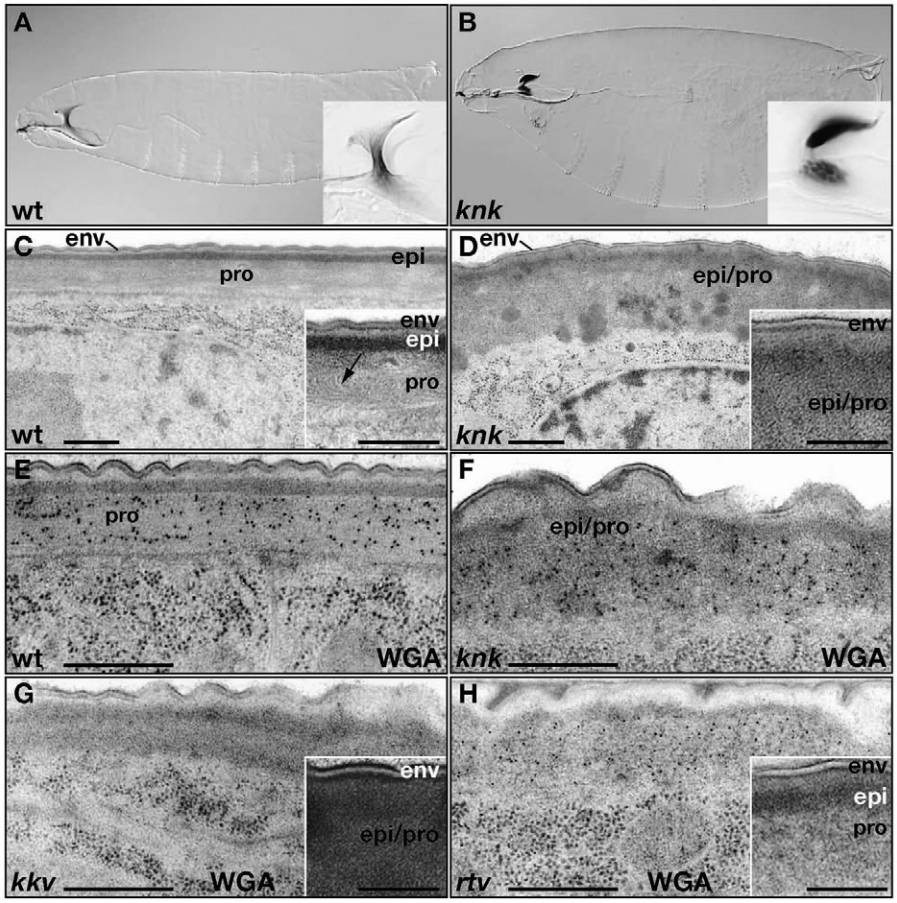

Fig. 4. Chitin is present in *knk* and *rtv* mutant procuticles, but lamellogenesis is defective. (**A**,**B**) Comparison of cuticle preparations of wild-type (A) and knk^{7A69}/knk^{5C77} (B) larvae shows that the *knk* cuticle is dilated and the *knk* head skeleton is strongly deformed and melanized (insets in A,B). (**C**,**D**) TEM analysis of cross-sections of wild-type (C) and knk^{5C77} mutant (D) larval cuticles reveals a defected epicuticle and procuticle in *knk* mutant larvae, but a normal envelope. The *knk* mutant procuticle is not clearly separable from the upper epicuticle (epi/pro), and inclusions of electron-dense material occupy the relicts of the procuticle. The *knk* procuticle is also devoid of chitin lamellar texture (arrow in inset in C, compare with inset in D). (**E**-**H**) Detection of chitin by gold-conjugated WGA (seen as black spots in the procuticle) reveals the presence of chitin in the wild-type procuticle (E), knk^{5C77} (F) and rtv^{11} (H) mutant procuticles, and not in kkv^{14D79} mutant cuticle (G). Insets in G and H illustrate fully contrasted magnifications of *rtv* and *kkv* cuticles to allow comparison with wild-type and *knk* cuticles in the insets in C and D. Scale bars: 0.5 μm; 0.25 μm in insets. env, envelope; epi, epicuticle; pro, procuticle.

In order to characterize the Knk protein further, we sequenced seven *knk* mutant alleles. All of these turned out to harbour base-pair changes that introduce premature translational stop codons (Fig. 5A). Mutants for knk^{7A69} and $knk^{50\text{-}12}$ are predicted to generate Knk proteins that lack the C-terminal GPI-signal, and display the same developmental defects as mutants for $knk^{3\text{-}7H}$, which encode a severely truncated 32 amino acid Knk protein (not shown). This suggests that the predicted GPI-anchor is essential for Knk function. In order to test whether Knk is a GPI-linked protein, we prepared wild-type embryonic lysate, removed the cellular debris, and separated the membrane fraction from the soluble portion. Both samples were analysed for the presence of Knk, using a polyclonal anti-Knk serum, and for the membrane-bound protein Syntaxin 1A (Syx1A) as a control. Knk was detected in both fractions, whereas Syx1A was present only in the membrane fraction. This indicates that Knk can exist both as a membrane-bound and a soluble protein. We next tested if the membrane-associated Knk protein could be released by treating the membrane fraction with Phospholipase C, which specifically cleaves GPI-linkages. Indeed, upon Phospholipase C treatment, some of the Knk protein was liberated into the soluble fraction. In control experiments without addition of Phospholipase C, no Knk protein was detected in the soluble fraction, indicating that Knk associates with the plasma membrane through a GPI-anchor (Fig. 5C).

Consistent with a requirement during tracheal morphogenesis and later, for cuticle production, the *knk* mRNA is detected in the developing trachea from stage 13, just before tube expansion, and in the epidermis from late stage 15 (Fig. 5D-F). The Knk protein is also found in the developing trachea (Fig. 5G) and the late epidermis (Fig. 5I), but appear absent in *knk* mutants (Fig. 5H,K,L). Double labelling with anti-Knk and the septate junction marker Fas3 further show that Knk mainly localize to the apical plasma membrane of these cells, being present along the apical and apico-lateral cell surfaces, and partly overlapping with the distribution of the Fas3 protein (Fig. 5I,J).

In order to test if the function of Knk requires its membrane-bound form, rather than a cleaved form of the protein released into the lumen, we asked whether *knk* mutant embryos can be rescued by expression of a transmembrane Knk protein. We first established that ubiquitous expression of a UAS-*knk* transgene driven by Tubulin-GAL4 rescues both *knk* lethality and the tracheal and cuticle *knk* defects (Fig. 5M,N and not shown). We then replaced the predicted GPI anchor of Knk with the transmembrane portion of the Transferrin receptor (CG10620). Expression of the resulting UAS-knk^{TM} in *knk* mutants using the same Tubulin-GAL4 driver also rescue both the *knk* tracheal phenotypes and lethality (Fig. 5O). Thus, membrane-bound Knk fulfils the requirements for Knk in tracheal tube expansion and cuticle deposition.

Knk is mislocalized in SJ mutants

The *knk* and *rtv* mutant phenotypes are also reminiscent of that of mutants with disrupted SJ components (‘SJ mutants’) (Beitel and Krasnow, 2000; Behr et al., 2003; Hemphala et al., 2003; Paul et al., 2003; Llimargas et al., 2004; Wu et al., 2004). SJ mutants display an overgrown DT at stage 15 with weak constrictions at fusion branches, convoluted dorsal trunks at stage 16 and discontinuous GB lumens (Beitel and Krasnow, 2000). As the luminal chitinous matrix is disorganized in SJ mutants, it was suggested that SJ components may function in tubulogenesis through their role in luminal matrix assembly (Tonning et al., 2005).

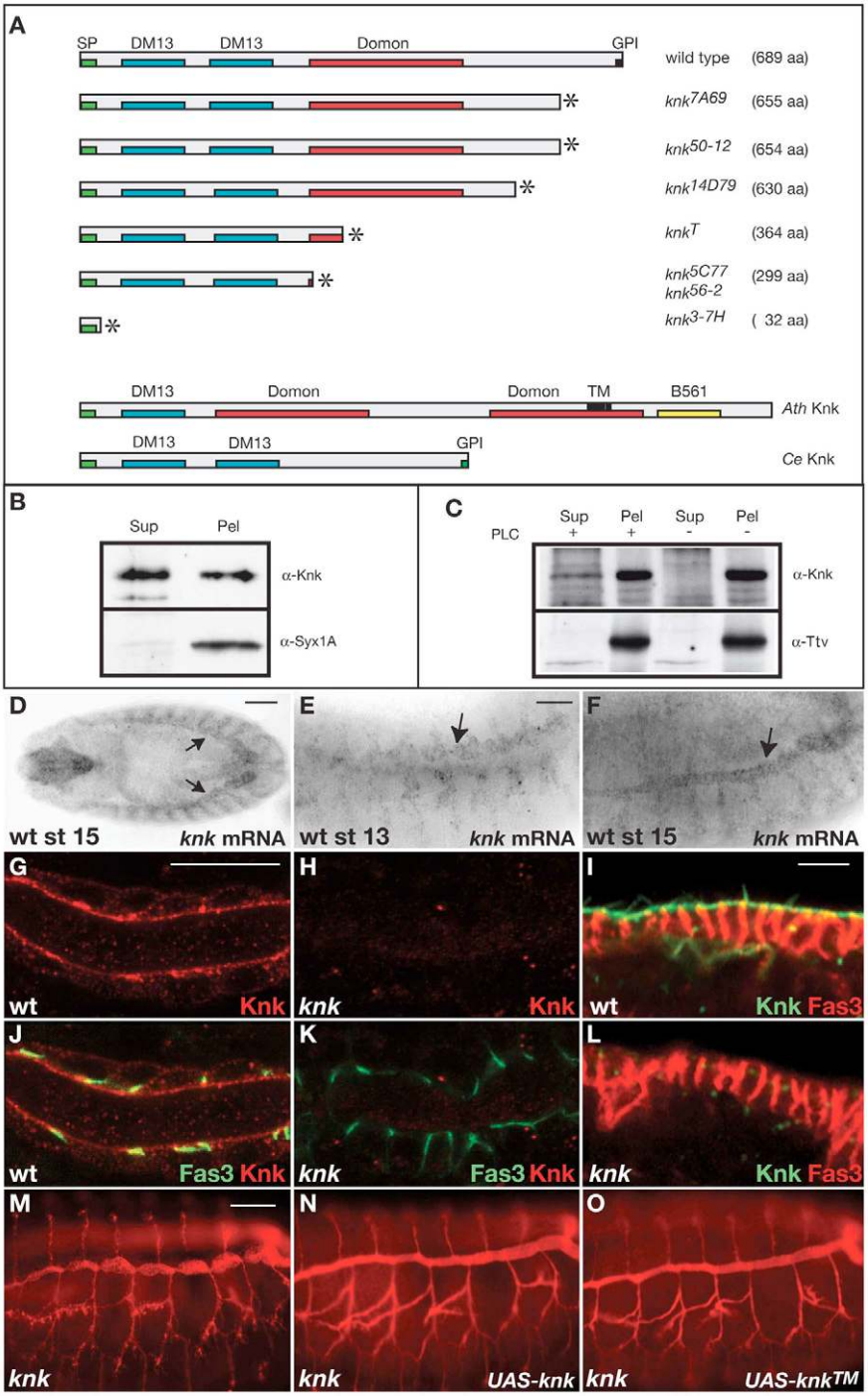

Fig. 5. Knk is an apical GPI-anchored protein expressed in the developing trachea and epidermis. (**A**) The wild-type Knk protein (top) is predicted to contain an N-terminal signal peptide (green), two tandem DM13 domains (blue), one DOMON (red) domain and a C-terminal GPI-anchor (black). Seven *knk* alleles, which all cause the same phenotypes, harbour premature stop codons to produce truncated Knk proteins of various lengths (illustrated below the wild Knk protein). The closest relatives to Knk in plant and worms are represented by *Arabidopsis thaliana* (Accession number BAB08762), with four transmembrane domains (TM, black) and a cytochrome BS61 domain (yellow), and *Caenorhabditis elegans* (Accession number AAG49388). (**B**) Western blot analysis of stage 17 embryonic extracts show that Knk protein is present in both the membrane (pel) and the soluble fraction (sup), compared with the transmembrane Syntaxin1A protein, which only precipitates with the membrane fraction. (**C**) Incubation of the membrane fraction in (B; pel) with Phospholipase C releases some Knk into the membrane-free supernatant (sup), indicating that Knk is a GPI-anchored protein. By contrast, Tout-velu (Ttv), which has a C-terminal type 1b transmembrane domain, is resistant to Phospholipase C treatment. (**D-F**) In-situ hybridization with *knk* anti-sense RNA probes detects *knk* transcripts in the developing trachea from stage 13 (arrows in D-F). From stage 15 the Knk transcript is also detected in the pharynx, hindgut and epidermis (D). (**G-L**) Co-labelling with anti-Knk and anti-Fas3 reveals apical Knk localization in the trachea and epidermis. In stage 15 wild type tracheal epithelium anti-Knk (G and J; red) highlights the apical cell surface and parts of the apico-lateral surface as seen from the slight overlap with Fas3 (J; green). Knk-labelling is absent in *knk* mutant trachea (H,K). Stage 16 wild-type epidermis (I) also displays apical Knk labelling (green) compared with the lateral Fas3 (red), which is absent in the *knk* mutant epidermis (L). (**M-O**) Stage 15 embryos labelled with the 2A12 antibody shows that the tracheal phenotype of *knk* mutants (M) is rescued by ectopic expression of *UAS-knk* (N) and *UAS-knk*^{TM} (O) driven with Btl-GAL4. Scale bars: 50 μm in D; 25 μm in E,F,M-O; 7 μm in G-L.

The requirement for both SJ components and Knk in chitin matrix formation prompted us to investigate the functional relationship between these proteins. First we analysed SJ integrity in *knk* mutant epithelia, by staining for the SJ proteins Fasciclin 3 (Fas3) and Discs large 1 (Dlg1), and found that *knk* mutants display normal levels and distribution of these markers (Fig. 6A-D). We also analysed the structure of the SJ junctions in *knk* mutants by TEM, which reveal indistinguishable SJ 'ladders' in these mutants compare with wild type (Fig. 6E,F). These results suggest that the composition of SJs is not affected in *knk* mutants. In addition, we confirmed that the *knk* mutant epithelia exhibit normal apical basal polarity upon labelling with the apical protein Crumbs (Tepass et al., 1990) (Fig. 6G,H).

In order to further address the functional relationship between Knk and SJs, we analysed double mutant combinations between *knk* and SJ mutants. When chitin deficiency is combined with SJ mutations, the embryos display a striking additive loss in relation to luminal 2A12 accumulation, indicating that SJ proteins may be needed for the deposition or stability of luminal components other than chitin (Tonning et al., 2005). We find that double mutants for *knk* and two SJ mutants, *Fas2* and *mega* (*pickel* – FlyBase), also display an additive reduction in luminal 2A12 levels (Fig. 6I-L and not shown), albeit not as strong as that observed in *Fas2;kkv* and *mega;kkv* double mutants. These cellular and genetic analyses further strengthen the idea that the requirement for Knk in tube-size regulation is specifically related to that of chitin.

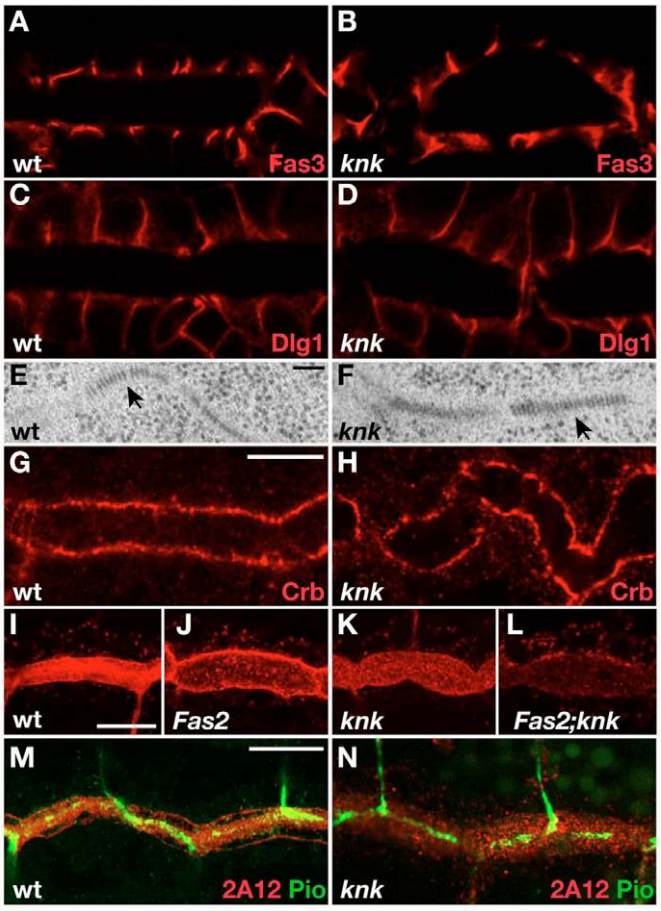

Fig. 6. Analysis of epithelial polarity and SJ integrity in *knk* mutants. (**A-D**) The *knk* mutant tracheal epithelium displays normal levels and distribution of the two SJ proteins Fas3 (B) and Dlg1 (D), compared with the wild type (A,C). (**E**,**F**) TEM analysis of wild-type (E) and *knk* mutant (F) epidermis reveals a normal 'ladder'-like SJ structure (arrows) in the mutants. (**G**,**H**) The apical marker Crumbs localizes normally along the apical cell surface in *knk* mutants (H), compared with the wild type (G). (**I**,**L**) Embryos homozygous for loss-of-function alleles of *Fas2* and *knk* display additive reduced luminal 2A12 levels. Early stage 15 wild-type (I), *Fas2* (J), *knk* (K) and *Fas2;knk* (L) mutant embryos labelled with antibody 2A12. The images were obtained with identical confocal settings, and show that luminal 2A12 levels are reduced in *Fas2* mutants, reduced and unevenly distributed in *knk* mutants and absent in *Fas2;knk*^{7A69} double mutants. The cellular 2A12 levels are, however, comparable. (**M**,**N**) The luminal Pio protein appears unaffected in *knk* mutant DT (N), compared with wild type (M), as shown by co-labelling for Pio (green) and 2A12 (red). Scale bars: 5 μm in A-D; 10 nm in E,F; 7 μm in G-N.

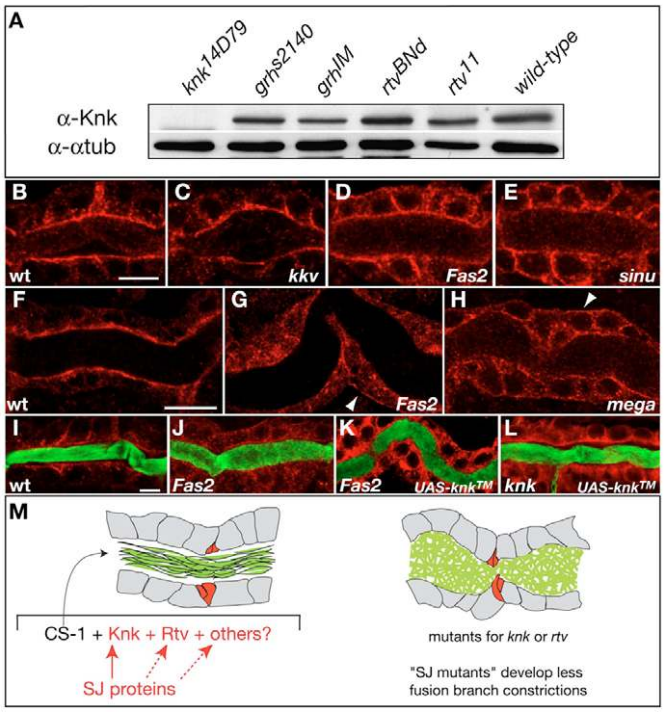

Fig. 7. Levels and localization of Knk in tube-expansion mutants. (**A**) A western blot with embryonic extract from stage 17 wild type and *knk*, *grh* and *rtv* mutants labelled with anti-Knk reveals similar Knk levels in embryos of all genotypes (top row). Anti-Tubulin was used for loading control (bottom row). (**B-E**) Anti-Knk labelling of stage 15 wild-type (B), *kkv* (C), *Fas2* (D) and *sinu* (E) mutant DTs shows that Knk localizes to the apical surface in wild type and *kkv* mutants, but occupies the entire cell surface in *Fas2* and *sinu* mutants. (**F-H**) Anti-Knk also labels the apical surface in wild-type stage 16 DT (F), but in *Fas2* (G) and *mega* (H) mutants Knk is detected along the lateral and basal cell surface (arrowhead). (**I-L**) *UAS-knk*^{TM}-expression, driven with the tracheal Btl-GAL4 line, rescues the *knk* (L), but not the *Fas2* (K) mutant tracheal phenotypes, as analysed by co-labelling with anti-Knk (red) and CBP (green). In *Fas2* mutants (J) luminal chitin appears amorphous and expanded compared with wild type (I), and *UAS-knk*^{TM}-expression in *Fas2* mutants (K) does not rescue chitin filament organization nor tube-size defects. (**M**) A model illustrating the requirement of different tube expansion genes for uniform lumen diameter expansion. Chitin chains (green) in the expanding lumen assemble into a filamentous cable in a process that requires the apical surface proteins Knk and Rtv, and perhaps additional components (left figure). SJ components are needed for the correct localization of Knk and possibly other proteins involved in chitin filament assembly. In *knk* and *rtv* mutants, chitin fails to assemble into a filamentous cable (right figure) and loses its function in tracheal tube-size regulation. Loss of SJ components also leads to defects in chitin matrix assembly, but not to the severe fusion branch constrictions seen in *knk* and *rtv* mutants. Scale bars: 4 μm in B-E,I-L; 5 μm in F-H.

Finally, we tested the levels and subcellular localization of Knk in tube-expansion mutants. Western blot analyses show that Knk levels in *rtv* and *kkv* mutants are comparable to those of wild type (Fig. 7A), and that the Knk protein localize normally to the plasma membrane of the apical cell domain in these two mutants (Fig. 7B,C and not shown). Knk levels are also normal in mutants for *grainy head* (*grh*), which disrupts a transcription factor essential for cuticle deposition and restricted tracheal tube elongation (Bray and Kafatos, 1991; Hemphala et al., 2003) (Fig. 7A), indicating that Grh is not a prerequisite for developmental Knk expression. Knk was, however, mislocalized in tube-expansion mutants, disrupting SJ components. In the five SJ mutants analysed, *Fas2*, *sinuous* (*sinu*), *mega*, *bulbous* (*Lachesin* – FlyBase) and *Na pump α subunit* (*ATPα*), Knk is distributed along the entire lateral and basal cell surfaces instead of concentrating at the apical tracheal epithelium (Fig. 7D-H and not shown), Thus, SJ proteins appear to be required for correct targeting of Knk to the apical surface, or to prevent its diffusion to other domains of the plasma membrane. In order to assess whether this Knk mislocalization is the cause for the tracheal tube size defects in SJ mutants, we tested if the *Fas2* and *mega* mutant luminal chitin matrix could be rescued by ectopic expression of transmembrane Knk. Ectopic expression of *UAS-knk*^{TM} in *Fas2* and *mega* mutant tracheal

epithelia was driven with the Btl-GAL4 driver-line, and was unable to restore their chitin-filament structure and tube size defects (Fig. 7I-L, and not shown). These results thus suggest that additional components necessary for chitin filament formation may be affected in SJ mutants.

DISCUSSION

We show that the two genes *rtv* and *knk* are required for chitin organization in the procuticle and tracheal lumen, pointing to a specific function for these proteins in chitin chain assembly that is crucial for tubulogenesis and integument differentiation.

Chitin filament assembly

In chitin-containing extracellular matrices, the chitin chains often bundle to form microfibrils. Such chitin chain bundling is mediated by hydrogen bonding of amine and carbonyl groups between the single sugar chains, and nascent chitin chains can spontaneously assemble into microfibrils. The insect cuticle predominately contains α-chitin, where ten or more polymers assemble in an anti-parallel orientation stabilized by a high number of hydrogen bonds to allow tight packaging (Kramer and Koga, 1986; Lehane, 1997; Merzendorfer, 2005). The fibrous appearance of the tracheal intraluminal matrix seen with CBP labelling also probably represents bundles of chitin microfilaments. This is strengthened by previous observations that Congo Red, a fluorescent dye that intercalates between hydrogen-bonded chitin chains (Cohen, 1993), visualizes luminal chitinous filaments that run parallel with tube length (Tonning et al., 2005). It is unclear whether the tracheal luminal chitin also exhibits an α-packaging like the procuticle. Alternatively, the luminal chitin may assume a softer and more flexible chitinous structure seen in the peritrophic matrix, in which the chains are aligned in a parallel fashion (β-form), involving fewer inter-chain hydrogen bonds but increased hydrogen bonding with water molecules that leads to its swelling (Peters, 1992; Merzendorfer, 2005).

Insect chitin synthases are large transmembrane proteins (Tellam et al., 2000; Merzendorfer and Zimoch, 2003), which produce and export chitin polymers to the extracellular space. We find that decreased chitin synthesis upon treatment with Nikkomycin alters the texture of the reduced luminal tracheal chitin, as it fail to present the characteristic fibrillar structure. It is thus tempting to speculate that a critical amount of localized chitin synthesis is required for chitin-chain bundling. The glycosyltransferases that form the glycosidic bonds in chitin, cellulose and hyaluronan belong to an evolutionarily conserved family of proteins (Yoshida et al., 2000; Coutinho et al., 2003; Merzendorfer, 2005), and cellulose synthases are found to function as oligomers, called rosettes, which are assembled in the Golgi and then transported to the plasma membrane (Richmond and Somerville, 2000; Saxena et al., 2001; Doblin et al., 2002). Each rosette consists of six synthesizing units, and the rosettes may align single cellulose chains before their spontaneous bundling to yield a microfibril. In a similar way, chitin synthases could function only after super-complex formation. If some of the chitin synthases in the complex were inhibited by Nikkomycin, there would be fewer strands synthesized in each complex that in turn could prevent microfilaments bundling.

The function of Knk and Rtv in chitin filament assembly

Based on genetic experiments and chitinous matrix analyses, we propose that Knk and Rtv are specifically needed for chitin filament assembly. As Knk, and possibly Rtv, associate with the external cell surface, and Knk can function also as a transmembrane protein, the two proteins are not likely to be part of the chitin matrices themselves. Instead, their requirements point to a role for the epithelial cell surface in organizing the extracellular chitinous matrix. No enzyme domains are detected in Knk and Rtv, and all the seven *knk* mutant alleles characterized introduce non-sense mutations, which is atypical for mutant alleles of genes that encode enzymes. It is thus likely that Knk and Rtv are structural proteins assisting in chitin filament assembly. Rtv exposes six aromatic residues that may bind to chitin (Moussian et al., 2005b), and the DOMON domain of Knk is predicted to form a Fibronectin type III-like (Fn3) fold that mediates extracellular adhesion (Aravind, 2001). Because chitin synthases, as discussed above, may need to assemble into higher order complexes to promote chitin microfibril formation, Knk and Rtv could assist in correct CS-1 cluster formation and chitin chain assembly through interactions with both CS-1 and chitin. Such a function may be analogous to that of Cobra, a plant apical GPI-linked protein required for oriented deposition of cellulose microfibrils and anisotropic cell expansion during plant morphogenesis (Roudier et al., 2005). Another possibility is that Knk and Rtv are needed for higher-order chitin matrix assemblies. The yeast exocellular protein Gas1, for example, is required for cell wall assembly and formation of cross-links between the cell wall glucans, possibly by catalyzing a transglycosylation reaction (Popolo and Vai, 1999). The localized activity of putative related enzymatic modifications of *Drosophila* chitin matrices could thus depend on apical Knk and Rtv. However, the enzyme Dopadecarboxylate, which is required for synthesis of the important cuticle cross-linking quinones, is not required for tracheal tube diameter expansion (not shown).

A role for tube expansion genes in chitin matrix formation

Several tracheal tube expansion mutants are identified that show various degrees of tube diameter defects and overgrown tracheal tube lengths (Beitel and Krasnow, 2000; Hemphala et al., 2003; Tonning et al., 2005). It appears that most of these mutants affect the luminal chitin filament, which is needed to coordinate tube diameter expansion and limit excess tube elongation. Apart from *kkv*, encoding CS-1, the major group of tube-expansion mutants disrupt SJ components and also affect luminal components and chitin filament structure (Wu and Beitel, 2004; Tonning et al., 2005). As the two new tube-expansion genes encoding Knk and Rtv appear specifically required for the ordered assembly of chitin filaments into a functional fibrous matrix, correct organization of the luminal chitin filament appears central for its role in uniform tube diameter growth. Bundling of luminal chitin may enable its uniform expansion upon lumen growth, which in turn promotes a uniform expansion of the surrounding epithelium. Without properly bundled chitin, as in mutants for *knk*, *rtv* and in SJ mutants, the chitinous matrix fills the entire lumen and appears to have lost its rigidity, and the lumen swells as if no or little matrix were present to shape the epithelium.

The mislocalization of Knk in mutants that disrupt SJ genes (*Fas2*, *bulb*, *sinu*, *ATPα* and *mega*), suggest that one role for SJs in tracheal tube expansion is to ensure luminal chitin filament organization through correct distribution of components involved in chitin filament assembly. Knk mislocalization is, however, not sufficient to explain the requirement for SJs in chitin matrix assembly, as overexpression of Knk in *Fas2* and *mega* mutants does not rescue the tracheal defects in these mutants, and it is plausible that the proper localization of additional components needed for chitin filament organization, for example Rtv, also are affected in SJ mutants. Mutants for *mega* and *bulb* display normal epithelial apico-basal polarity (Behr et al., 2003; Llimargas et al., 2004). Their defects in polarized protein localization

may thus expose a need for SJs in protein export to the correct cell membrane domain, or in preventing diffusion of proteins between the apical and baso-lateral compartments.

We thank Markus Affolter for providing the Pio antiserum, York Stierhof (ZMBP, Tübingen) for gold-conjugated protein A, Slawek Bartozsewski for sharing *knk* mutant strains, Inge The for anti-Ttv, Ursel Müller and Christof Seifarth for technical assistance, and Swegene Centre for Cellular Imaging at Gothenburg University for use of imaging equipment. The antibodies obtained from the Developmental Studies Hybridoma Bank developed under the auspices of the NICHD and maintained by the University of Iowa, Department of Biological Sciences, Iowa City, IA 52242 were developed by Drs Knust and Goodman. We also thank Christos Samakovlis, in whose laboratory the tracheal analysis of *knk* and *rtv* mutants was initiated. The work was supported by grants from the Swedish Research Council and Åke Wibergs funds to A.U. B.M. was supported by the Max-Planck Institute.

References

Aravind, L. (2001). DOMON: an ancient extracellular domain in dopamine beta-monooxygenase and other proteins. *Trends Biochem. Sci.* **26**, 524-526.
Bakkers, J., Kramer, C., Pothof, J., Quaedvlieg, N. E., Spaink, H. P. and Hammerschmidt, M. (2004). Has2 is required upstream of Rac1 to govern dorsal migration of lateral cells during zebrafish gastrulation. *Development* **131**, 525-537.
Behr, M., Riedel, D. and Schuh, R. (2003). The claudin-like megatrachea is essential in septate junctions for the epithelial barrier function in Drosophila. *Dev. Cell* **5**, 611-620.
Beitel, G. J. and Krasnow, M. A. (2000). Genetic control of epithelial tube size in the Drosophila tracheal system. *Development* **127**, 3271-3282.
Bray, S. J. and Kafatos, F. C. (1991). Developmental function of Elf-1: an essential transcription factor during embryogenesis in Drosophila. *Genes Dev.* **5**, 1672-1683.
Cabib, E. (1991). Differential inhibition of chitin synthetases 1 and 2 from Saccharomyces cerevisiae by polyoxin D and nikkomycins. *Antimicrob. Agents Chemother.* **35**, 170-173.
Cohen, E. (1993). Chitin synthesis and degradation as targets for pesticide action. *Arch. Insect Biochem. Physiol.* **22**, 245-261.
Cohen, E. (2001). Chitin synthesis and inhibition: a revisit. *Pest Manag. Sci.* **57**, 946-950.
Coutinho, P. M., Deleury, E., Davies, G. J. and Henrissat, B. (2003). An evolving hierarchical family classification for glycosyltransferases. *J. Mol. Biol.* **328**, 307-317.
Doblin, M. S., Kurek, I., Jacob-Wilk, D. and Delmer, D. P. (2002). Cellulose biosynthesis in plants: from genes to rosettes. *Plant Cell Physiol.* **43**, 1407-1420.
Ghabrial, A., Luschnig, S., Metzstein, M. M. and Krasnow, M. A. (2003). Branching morphogenesis of the Drosophila tracheal system. *Annu. Rev. Cell Dev. Biol.* **19**, 623-647.
Grenningloh, G., Rehm, E. J. and Goodman, C. S. (1991). Genetic analysis of growth cone guidance in Drosophila: fasciclin II functions as a neuronal recognition molecule. *Cell* **67**, 45-57.
Hemphala, J., Uv, A., Cantera, R., Bray, S. and Samakovlis, C. (2003). Grainy head controls apical membrane growth and tube elongation in response to Branchless/FGF signalling. *Development* **130**, 249-258.
Jazwinska, A., Ribeiro, C. and Affolter, M. (2003). Epithelial tube morphogenesis during Drosophila tracheal development requires Piopio, a luminal ZP protein. *Nat. Cell Biol.* **5**, 895-901.
Jurgens, G., Wieschaus, E., Nusslein-Volhard, C. and Kluding, H. (1984). Mutations affecting the pattern of the larval cuticle in Drosophila melanogaster. *Roux Arch. Dev. Biol.* **193**, 283-295.
Kramer, K. and Koga, D. (1986). Insect chitin: Physical state, synthesis, degradation and metabolic regulation. *Insect Biochem.* **16**, 851-877.
Lehane, M. J. (1997). Peritrophic matrix structure and function. *Annu. Rev. Entomol.* **42**, 525-550.
Llimargas, M., Strigini, M., Katidou, M., Karagogeos, D. and Casanova, J. (2004). Lachesin is a component of a septate junction-based mechanism that controls tube size and epithelial integrity in the Drosophila tracheal system. *Development* **131**, 181-190.
Merzendorfer, H. (2005). Insect chitin synthases: a review. *J. Comp. Physiol. B*, 1-15 [E-pub ahead of print].
Merzendorfer, H. and Zimoch, L. (2003). Chitin metabolism in insects: structure, function and regulation of chitin synthases and chitinases. *J. Exp. Biol.* **206**, 4393-4412.
Moore, K. L. (2003). The biology and enzymology of protein tyrosine O-sulfation. *J. Biol. Chem.* **278**, 24243-24246.
Moussian, B., Schwarz, H., Bartoszewski, S. and Nusslein-Volhard, C. (2005a). Involvement of chitin in exoskeleton morphogenesis in Drosophila melanogaster. *J. Morphol.* **264**, 117-130.
Moussian, B., Soding, J., Schwarz, H. and Nusslein-Volhard, C. (2005b). Retroactive, a membrane-anchored extracellular protein related to vertebrate snake neurotoxin-like proteins, is required for cuticle organization in the larva of Drosophila melanogaster. *Dev. Dyn.* **233**, 1056-1063.
Ostrowski, S., Dierick, H. A. and Bejsovec, A. (2002). Genetic control of cuticle formation during embryonic development of Drosophila melanogaster. *Genetics* **161**, 171-182.
Paul, S. M., Ternet, M., Salvaterra, P. M. and Beitel, G. J. (2003). The Na+/K+ ATPase is required for septate junction function and epithelial tube-size control in the Drosophila tracheal system. *Development* **130**, 4963-4974.
Peters, W. (1992). *Peritrophic membranes: Zoophysiology Series*, vol. 30. Berlin: Springer-Verlag.
Popolo, L. and Vai, M. (1999). The Gas1 glycoprotein, a putative wall polymer cross-linker. *Biochim. Biophys. Acta* **1426**, 385-400.
Richmond, T. A. and Somerville, C. R. (2000). The cellulose synthase superfamily. *Plant Physiol.* **124**, 495-498.
Roudier, F., Fernandez, A. G., Fujita, M., Himmelspach, R., Borner, G. H., Schindelman, G., Song, S., Baskin, T. I., Dupree, P., Wasteneys, G. O. et al. (2005). COBRA, an Arabidopsis extracellular glycosyl-phosphatidyl inositol-anchored protein, specifically controls highly anisotropic expansion through Its involvement in cellulose microfibril orientation. *Plant Cell* **17**, 1749-1763.
Samakovlis, C., Hacohen, N., Manning, G., Sutherland, D. C., Guillemin, K. and Krasnow, M. A. (1996). Development of the Drosophila tracheal system occurs by a series of morphologically distinct but genetically coupled branching events. *Development* **122**, 1395-1407.
Saxena, I. M., Brown, R. M., Jr and Dandekar, T. (2001). Structure–function characterization of cellulose synthase: relationship to other glycosyltransferases. *Phytochemistry* **57**, 1135-1148.
Shiga, Y., Tanaka-Matakutsu, M. a. and Hayashi, S. (1996). A nuclear GFP/b-galactosidase fusion protein as a marker for morphogenesis in living *Drosophila*. *Dev. Growth Differ.* **38**, 99-106.
Spicer, A. P. and Tien, J. Y. (2004). Hyaluronan and morphogenesis. *Birth Defects Res. Part C Embryo Today* **72**, 89-108.
Spradling, A. C., Stern, D., Beaton, A., Rhem, E. J., Laverty, T., Mozden, N., Misra, S. and Rubin,G. M. (1999). The Berkeley Drosophila genome project gene disruption project. Single P-element insertions mutating 25% of vital Drosophila genes. *Genetics* **153**, 135-177.
Tellam, R. L., Vuocolo, T., Johnson, S. E., Jarmey, J. and Pearson, R. D. (2000). Insect chitin synthase cDNA sequence, gene organization and expression. *Eur. J. Biochem.* **267**, 6025-6043.
Tepass, U., Theres, C. and Knust, E. (1990). crumbs encodes an EGF-like protein expressed on apical membranes of Drosophila epithelial cells and required for organization of epithelia. *Cell* **61**, 787-799.
Tonning, A., Hemphala, J., Tång, E., Nannmark, U., Samakovlis, C. and Uv, A. (2005). A transient luminal chitinous matrix is required to model epithelial tube diameter in the *Drosophila* trachea. *Dev. Cell* **3**, 423-430.
Toole, B. P. (2004). Hyaluronan: from extracellular glue to pericellular cue. *Nat. Rev. Cancer* **4**, 528-539.
Uv, A., Cantera, R. and Samakovlis, C. (2003). Drosophila tracheal morphogenesis: intricate cellular solutions to basic plumbing problems. *Trends Cell. Biol.* **13**, 301-309.
Wieschaus, E. and Nüsslein-Volhard, C. (1986). Looking at embryos. In *Drosophila: A Practical Approach* (ed. D. B. Roberts), pp. 199-227. Oxford: IRL Press.
Wieschaus, E., Nusslein-Volhard, C. and Jurgens, G. (1984). Mutations affecting the pattern of the larval cuticle in Drosophila melanogaster. *Roux Arch. Dev. Biol.* **193**, 196-307.
Wu, V. M. and Beitel, G. J. (2004). A junctional problem of apical proportions: epithelial tube-size control by septate junctions in the Drosophila tracheal system. *Curr. Opin. Cell Biol.* **16**, 493-499.
Wu, V. M., Schulte, J., Hirschi, A., Tepass, U. and Beitel, G. J. (2004). Sinuous is a Drosophila claudin required for septate junction organization and epithelial tube size control. *J. Cell Biol.* **164**, 313-323.
Yoshida, M., Itano, N., Yamada, Y. and Kimata, K. (2000). In vitro synthesis of hyaluronan by a single protein derived from mouse HAS1 gene and characterization of amino acid residues essential for the activity. *J. Biol. Chem.* **275**, 497-506.